CREEP OF PRECIPITATION-STRENGTHENED Al(Sc) ALLOYS

EMMANUELLE A. MARQUIS, DAVID N. SEIDMAN, DAVID C. DUNAND
Department of Materials Science and Engineering, Northwestern University, Evanston, IL, 60208, USA

We studied the effect of precipitate radius and volume fraction upon yield and creep strength of dilute Al-Sc alloys in the temperature range 225 to 300°C. Coherent, spheroidal Al_3Sc precipitates in alloys with 0.10 to 0.30 wt.% Sc (corresponding to precipitate volume fractions in the range 0.23 to 0.68%) were grown to radii in the range 1.4 to 9.5 nm through various heat-treatments. Creep threshold stresses were found to be about ten times lower than the yield stresses at 300°C, indicative of a climb-controlled bypass mechanism, which is modeled according to existing theories. Transmission electron microscopy observations of deformed samples illustrate the interactions between dislocations and precipitates.

Creep Deformation: Fundamentals and Applications
Edited R.S. Mishra, J.C. Earthman and S.V. Raj
TMS (The Minerals, Metals & Materials Society), 2002

Introduction

Al-Sc alloys have excellent mechanical properties at room temperature, due to the presence of coherent Al_3Sc precipitates that can be obtained at a very high number density, thus blocking mobile dislocations and stabilizing fine-grain structures [1]. These Al_3Sc precipitates are stable against coarsening up to temperatures as high as 350°C [2], which constitutes a significant enhancement in comparison to commercial age-hardenable aluminum alloys [3]. At elevated temperatures, most studies report that Al-Sc alloys have good superplastic properties [4, 5] because the stable Al_3Sc precipitates stabilize very fine grain sizes, which leads to rapid diffusional creep. Only one study concerns itself with coarse-grained Al-Sc alloys, where the creep behavior of two Al-Sc alloys containing low volume fractions of Al_3Sc precipitates was investigated and threshold stresses for creep at 300°C were measured [6]. The present paper reports a systematic study of the yield and creep behavior in aluminum alloys containing low volume-fractions of Al_3Sc precipitates (less than 0.74 vol.%) at temperatures between 225 and 300°C.

Experimental Procedures

Materials preparation and heat-treatments. Billets of aluminum with 0.10, 0.15, 0.20 or 0.30 wt.% Sc were prepared by melting in air appropriate amounts of 99.9% pure Al and an Al-1.2 wt.% Sc master alloy and casting into a graphite mold. Heat-treatments consisted of homogenization in air at 648°C for 24 hr, water-quenching to room temperature, and aging in air at 300°C, terminated by water quenching. Some of the samples underwent double-aging treatments, e.g., aging at 300°C for 5 hr, water quenching followed by aging at 400°C for times between 3 to 11 hr.

Mechanical properties. Tensile creep tests were performed in air under constant stress (5 to 50 MPa) at constant temperature in the range of 225 to 300°C, i.e., at homologous temperatures T/T_m = 0.50 to 0.64 (where T_m is the absolute melting temperature of pure aluminum). After steady-state deformation was reached and the strain rate measured by extensometry, the load was increased, resulting in three to five data points for each sample.

Microstructural observation. Conventional transmission electron microscopy (TEM) was performed on an Hitachi 8100 operated at 200 kV. TEM was performed both before and after heat-treatment to examine precipitate radius, shapes, and interface coherency, as well as the dislocation structures. Some of the creep experiments were interrupted in the steady-state regime by cooling rapidly under load to room temperature, in order to maintain the dislocation structure developed during creep. Slices, 350 μm in thickness, were cut from the creep specimen gauge lengths perpendicular to the direction of the applied load. The slices were mechanically polished to a thickness of 200 μm, and twinjet electro-polished with a solution of 5% perchloric acid in methanol at –30°C.

Results

Initial microstructure. The cast and annealed alloys are coarse-grained, with a typical equiaxed grain size of 1 to 2 mm, independent of scandium concentration. The absence of primary precipitates was checked by scanning electron microscopy on polished sections. No

subgrains were observed by TEM in the microstructure of the alloys before creep deformation. A high number density of nearly spherical Al_3Sc precipitates was formed as a result of all aging treatments. These precipitates are coherent with the Al matrix, since coherency contrast was visible and no interfacial dislocations were observed. Representative TEM micrographs (Figs.1a and 1b) show the effect of temperature on the precipitate number density and size for the Al-0.3 wt.% Sc alloy. For a constant aging time, as the aging temperature increases, the average precipitate size increases and the number density of precipitates decreases. The effect of composition is illustrated by Figs. 1a and 1c, which show a decreasing number density (by a factor of about 200) and increasing precipitate radius (from 1.4 nm to 9 nm), when the scandium concentration is decreased from 0.3 to 0.1 wt.% Sc for the same aging conditions. The strain contrast due to coherent interfaces is illustrated in Fig. 1d.

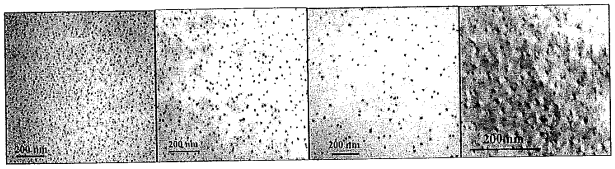

Figure 1: Dark-field TEM micrographs: (a) Al-0.3 wt.% Sc alloy aged at 300°C for 72 hr; (b) Al-0.3 wt.% Sc alloy aged at 400°C for 5 hr; (c) Al-0.1 wt.% Sc alloy aged at 300°C for 72 hr; and (d) coherency contrast in the Al-0.2 wt.% Sc alloy aged at 300°C for 72 hr.

When aging the Al-0.3 wt.% Sc alloy at 400°C, precipitate-free zones (PFZ) were observed near grain boundaries on which large, incoherent precipitates form, as shown in Fig.2. Because these precipitate free-zones are detrimental for the mechanical properties of Al alloys [7], double-aging treatments (e.g., 300°C for 5 hr followed by 400°C from 3 to 10 hr), were chosen to produce precipitates within the grains and limit the amount of grain boundary precipitation in creep samples. Precipitates are expected to nucleate during the first aging at 300°C and to coarsen during the subsequent aging treatment at 400°C.

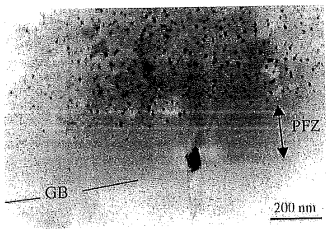

Figure 2: Dark-field TEM micrograph of a precipitate-free zone (PFZ) at a grain boundary in an Al-0.3 wt.% Sc alloy aged at 400°C for 5 hr. A large incoherent precipitate is also visible at the grain boundary.

High-temperature mechanical properties. At 300°C and a deformation rate of 0.02 s^{-1}, a yield strength of 101±5 MPa is measured for the Al-0.15 wt.% Sc alloy aged at 300°C for 5 hr and 400°C for 1 hr. After subsequent aging at 400°C for 7 hr, the yield strength at 300°C decreases to 57±6 MPa.

A normal primary creep region, where the strain rate decreases continuously, always preceded the steady-state creep regime. All specimens deformed to fracture under various stress levels exhibited more than 10% strain, with the exception of the Al-0.3 wt.% Sc alloy aged at 400°C, which exhibited only 4% deformation and brittle-like fracture along grain boundaries. Despite the very low scandium concentration levels, all alloys exhibit significant improvements in creep resistance at 300°C as compared to pure aluminum (Fig. 3a and b). In the experimental range of strain rates ($3x10^{-9}$ to $3x10^{-4}$ s^{-1}), high stress exponents were measured, decreasing from n = 24-30 at strain rates below $10^{-7}s^{-1}$, to n = 9-14 at higher strain rates. Two of the alloys (Al-0.3 wt.% Sc and Al-0.2 wt.% Sc) were tested at various temperatures between 225 and 300°C. Results for these alloys are presented in Figs. 3. The same peak aging treatment (300°C for 6 hr) was used for all specimens. Both the stress exponents and activation energies are high, the latter varying from 230 to 320 kJ/mol.

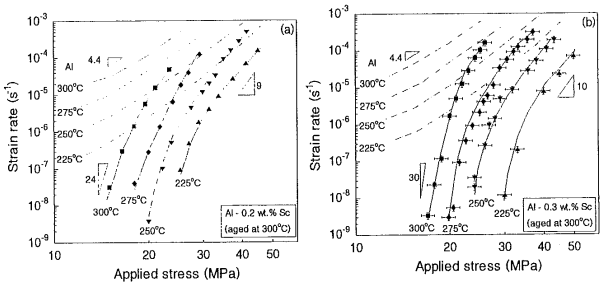

Figure 3: Effect of test temperature on creep behavior: (a) Al-0.2 wt.% Sc; and (b) Al-0.3 wt.% Sc. Both alloys were peak-aged at 300°C for 6 hr.

Finally, the alloys were creep-tested at 300°C after various heat-treatments between 300 and 400°C, providing a range of precipitate radii [2], to study the effect of precipitate radius upon the steady-state creep rate. Figure 4 shows that the creep resistance of the Al-0.3 wt.% Sc alloy increases with increasing Al_3Sc precipitate radius.

Deformed microstructure. In all deformed creep specimens, dislocations pinned at Al_3Sc precipitates were observed, suggesting strong dislocation-precipitate interactions. The dislocation structure developed during creep was examined in the Al-0.3 wt.% Sc alloy aged at 300°C for 5 hr. As seen in Fig. 5a, dislocation walls separate subgrains with a low dislocation density. Alternatively, in the same alloy containing larger precipitates (due to subsequent aging at 400°C for 7 h), no subgrains were observed (Fig. 5b).

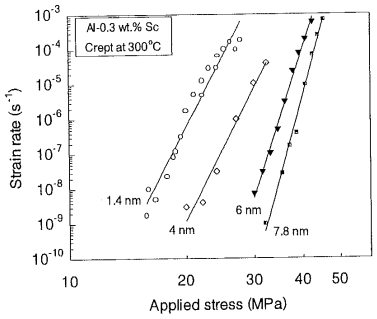

Figure 4: Strain rate versus applied stress for the Al-0.3 wt.% Sc alloy containing precipitates of average radii ranging from 1.4nm to 7.8 nm.

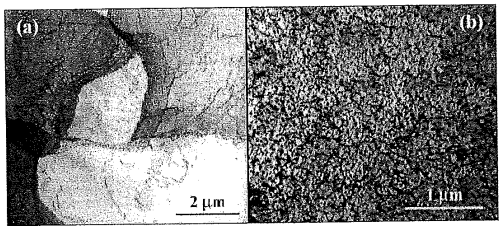

Figure 5: TEM micrographs of post-creep dislocation structures in: (a) Al-0.3 wt.% Sc alloy aged at 300°C for 5 hr, crept at 300°C under 22 MPa; and (b) Al-0.3 wt.% Sc alloy aged at 300°C for 5 hr and 400°C for 7 hr and then crept at 300°C under 36 MPa.

Discussion

Initial microstructure. The aging treatments produce Al_3Sc precipitates with an $L1_2$ structure, which are coherent with the matrix (Fig. 1d). The precipitate radius increases with increasing annealing time as a result of coarsening. For equal aging times, the average precipitate radius also increases with aging temperature due to a decreasing number density of precipitates and faster diffusion of Sc in Al [2]. The measured distributions agree with our previous study on the microstructure of Al(Sc) alloys in the same range of composition [2]. The Al_3Sc precipitates remain coherent for radii smaller than about 10 nm, for the heat-treatments used in this study. The presence of PFZs after aging at 400°C indicates that heterogeneous nucleation at grain boundaries becomes easier as the aging temperature increases, while the homogeneous

nucleation current decreases because of the lower Sc supersaturation. As observed in Al-Li alloys [8], heterogeneous nucleation at grain boundaries is then favored and a PFZ is formed near grain boundaries as solute atoms diffuse to the boundary precipitates.

Tensile tests. The heat-treatments used for the Al-0.15 wt.% Sc alloy produced an average precipitate radius from 3.6 to 8 nm. The predicted Orowan yield stress at 300°C is in close agreement with the experimental values. As expected, the yield stress decreases with the increasing precipitate radius, as the inter-precipitate distance increases at constant precipitate volume fraction. The increase in yield strength due to Orowan dislocation looping is given by Ref. [9]:

$$\Delta\sigma_{Or} = M\frac{0.813}{\pi}\frac{Gb}{\sqrt{1-\nu}}\frac{\ln\left(\frac{2\bar{r}}{b}\right)}{\lambda - 2\bar{r}} \quad ; \qquad (1)$$

where M = 3.06 is the mean matrix orientation factor (average Taylor factor) for aluminum [10], b = 0.286 nm is the magnitude of the Burger's vector [11], G = 21.1 GPa is the matrix's shear modulus at 300°C, λ is the inter-precipitate distance, $\bar{r} = 0.82r$ is the mean radius of the intersections of parallel planes with spherical precipitates of mean radius r, assuming an Lifshitz-Slyozov-Wagner distribution of particle radii [12], and $\nu = 0.34$ is Poisson's ratio [10]. The inter-precipitate spacing, λ, is taken as the square lattice spacing in parallel planes and is given by Ref. [12] as:

$$\lambda = \left[\left(\frac{\pi}{f}\right)^{1/2} - 2\right]\bar{r}; \qquad (2)$$

where f is the volume fraction of precipitates.

Creep experiments. First, the creep performances obtained in the present study, as compared to those obtained by Fuller et al. [6], are discussed based on differences in microstructure. Their first alloy, containing 0.07 wt.% Sc and aged at 350°C, exhibited larger Al_3Sc precipitates than in the present study (estimated to be about 15 nm in radius [2] and with probable partial loss of coherency), resulting in a very low number density of precipitates and therefore a weak strengthening effect. Their second alloy, with 0.21 wt.% Sc, and an estimated precipitate radius of 4 nm [2], has a comparable creep strength to the corresponding alloy in our study.
Because the grain size of the cast alloys is large, the operating mechanism for creep deformation is power-law creep by dislocation motion [11]. At low strain rates, the improved creep resistance of the alloys compared to pure aluminum suggests a strong interaction between precipitates and dislocations. The high values of the creep exponent can be interpreted as resulting from a threshold stress below which creep rates are negligible. This behavior is described by a modified creep equation, containing a threshold stress, σ_{th} [13]:

$$\dot{\varepsilon} = A\frac{DGb}{kT}\left(\frac{\sigma - \sigma_{th}}{G}\right)^{n}; \qquad (3)$$

where A is the Dorn constant, $D = D_0\exp(-Q/RT)$ is the diffusion coefficient of the matrix with Q, an activation energy, n = 4.4 is the matrix stress exponent, k is Boltzmann's constant, T is the absolute temperature and σ is the applied stress. According to Eq. 3, threshold stress values can be determined from linear plots of the strain rate raised to the power n^{-1} versus applied stress. Threshold stress values are given in Table I for all alloys studied[EM1]. Activation energies, corrected according to Eq. 3, can then be obtained from the slope of semi-logarithmic plots of strain-rate versus inverse-temperature at constant effective applied stress, σ-σ_{th}. The experimental values for the effective activation energies are 138±2 kJ/mol for the Al-0.3 wt.% Sc alloy and 120±8 kJ/mol for the Al-0.2 wt.% Sc alloy, calculated at σ-σ_{th} = 4-15 MPa.

Four possible mechanisms have been considered in the literature to explain the presence of threshold stresses in precipitation- or dispersion-strengthened metals [13]: (a) precipitate shearing; (b) Orowan dislocation looping; (c) dislocations climbing over precipitates; and (d) dislocation detachment, which is not active for coherent precipitates [14].

The corrected activation energy does not provide information on the controlling deformation mechanism since, if precipitate shearing is the controlling mechanism, the expected creep activation energy would be similar to that for creep of single-phase Al_3Sc, (128 kJ/mol [15]). If dislocation climb, which is diffusion limited in the aluminum matrix, is the rate controlling mechanism, the activation energy should be equal to the value for creep in Al (132 kJ/mol). The small numerical difference between these values does not allow any distinction of the operating mechanism, given the average experimental value of 129 kJ/mol. The shearing mechanism, however, can be excluded since it would lead to yield stress values that are higher by at least one order of magnitude than the observed threshold stress. The Orowan looping mechanism can be excluded for the same reason, the discrepancy being a factor of 2 to 17 (Table 2). A dislocation climb process is therefore considered since it requires lower stresses than the Orowan value, σ_{or} [13].

The threshold stress for climb originates from the increase in dislocation line length as dislocations climb over precipitate. Different values for the threshold stress are predicted depending on the details of the climb geometry adopted. Local climb (where the dislocation line between the precipitates remains in the glide plane) leads to a normalized threshold stress of $\beta = \sigma_{th}/\sigma_{or} = 0.4$, independent of the precipitate radius. Because the local climb process assumes a sharp bend at a precipitate interface, which can be relaxed by diffusion, general climb models, which are associated with smaller threshold stresses were developed. In the case of the Al(Sc) alloys studied, the normalized threshold stress β predicted by the above equations (solved numerically in a manner similar to that developed by Rosler and Arzt) is independent of the mean precipitate radius and is about 0.02-0.04. However, as shown in Fig. 5, the experimental values of β increase from 0.08 to 0.52, with the precipitate radius increasing from 1.4 to 9.6 nm. Because local climb with $\beta = 0.4$ is unstable, the accepted view is that only general climb with $\beta = 0.04$ is possible for coherent precipitates without a detachment stress. Therefore, the experimental results of $\beta = 0.04$-0.4 shown in Fig. 5 can only be explained if another particle-radius dependent mechanism contributes to the threshold stress. Modeling is under way to address this issue [16].

Table I: Dependence on the scandium concentration, heat-treatment, precipitate volume fraction, f, average precipitate radius, r, and inter-precipitate spacing, λ, of the threshold stress, σ_{th}, and the Orowan stress, σ_{Or}.

Alloy (wt.% Sc)	Heat-treatment	f* (%)	r (nm)	λ** (nm)	σ_{th} (MPa)	σ_{Or} *** (MPa)
0.1	300°C, 24 h	0.234	8.5 ± 0.65	256	19	38
0.1	275°C, 66 h	0.238	4.1 ± 0.4	123	8	64
0.2	300°C, 5 h	0.475	3 ± 0.3	62	14	115
0.2	350°C, 5 h	0.464	4.5 ± 0.4	94	16	87
0.2	300°C-5 h, 400°C-2 h	0.449	5.8 ± 0.5	128	22	71
0.3	300°C, 5 h	0.706	1.4 ± 0.25	23	17	225
0.3	350°C, 24 h	0.696	4.3 ± 0.4	67	22	112
0.3	300°C-5 h, 400°C-3 h	0.674	5.9 ± 0.5	102	28	88
0.3	300°C-5 h, 400°C-7 h	0.674	7.8 ± 0.65	136	31	70
0.3	300°C-5 h, 400°C-10 h	0.674	9.6 ± 0.8	154	32	62

* From lever rule and equilibrium Al-Sc phase diagram between 300 and 400°C [17]
** From Eq. 2
*** From Eq. 1 (calculated at 300°C).

Deformed microstructure. Different crept microstructures were observed according to the average precipitate radius. For small precipitate radius (Al-0.3 wt.% Sc aged at 300°C for 6 hr), formation of subgrains is observed, as shown in Fig. 5a. For small precipitates, dislocations climb rapidly over the precipitates, so that the deformed microstructure is very similar to observations of crept Al samples [18], where the subgrain size, ω, can be related to the applied stress through [19]:

$$\omega = 28b\frac{G}{\sigma}. \qquad (4)$$

Equation 4 predicts $\omega \approx 9$ μm for an applied stress of 20 MPa at 300°C, in agreement with the present observations. For larger precipitates, the dislocations are pinned more efficiently by precipitates as dislocation climb becomes slower. No subgrains are observed but a uniform distribution of tangled dislocations, which are pinned at precipitates (Fig. 5b).

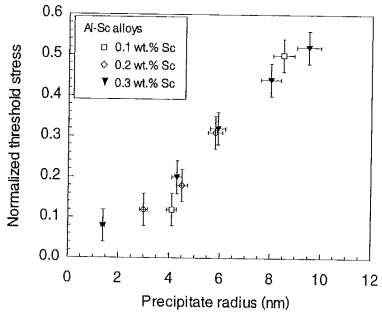

Figure 6: The creep threshold stress normalized by the Orowan stress at 300°C for all alloys and conditions tested versus the average precipitate radius.

Conclusions

Precipitation strengthening of Al with 0.1 to 0.3 wt.% Sc was studied at elevated temperatures with the following conclusions:

- Heat-treatments at temperatures between 275 and 400°C resulted in coherent, spheroidal $L1_2$ Al_3Sc precipitates with a mean radius between 1.4 to 9.5 nm.
- A creep threshold stress in the range 8-32 MPa is found for the alloys tested at 300°C, with an activation energy (measured between 225 and 300°C) of 129 kJ/mol, very close to that for creep of pure matrix or the Al_3Sc phase.
- The threshold stress increases linearly with increasing precipitate radius, from 0.08 σ_{Or} at 1.4 nm to 0.52 σ_{Or} at 9.5 nm, where σ_{Or} is the Orowan stress. Existing threshold stress models are being modified to account for the precipitate radius dependence of the threshold stress for creep.

Acknowledgments - This research is supported by the United States Department of Energy, Basic Energy Sciences Division, under contract DE-FG02-98ER45721. The authors acknowledge Ashurst Corp. for kindly supplying the Al(Sc) master alloy.

References

1. Toporova L.S., Eskin D.G., Kharakterova M.L., and Dobatkina T.B., Advanced Aluminum Alloys Containing Scandium (Gordon & Breach: Amsterdam, 1998).

2. Marquis E.A. and Seidman D.N., "Nanoscale structural evolution of Al3Sc precipitates in Al(Sc) alloys," Acta Mater. 49 (2001), 1909.

3. Drits M.Y., "Ageing of alloy Al-0.3 at%Sc," Phys.Met.Metall. 57 (6) (1984), 118-126.

4. Sawtell R.R. and Jensen C.L., "mechanical properties and microstructure of Al-Mg-Sc alloys," Met. Trans. 21A (1990), 421-430.

5. Nieh T.G., Hsiung L.M., Wadsworth J., and Kaibyshev R., "High strain rate superplasticity in a continuously recrystallized Al-6%Mg-0.3%Sc alloy," Acta mater. 46 (8) (1998), 2789.

6. Fuller C.B., Seidman D.N., and Dunand D.C., "Creep properties of Al(Sc) alloys at 300C," Scripta metall. 40 (1999), 691.

7. Sanders T.H. and Starke Jr E.A., "The effect of slip distribution on the monotonic and cyclic ductility of Al-Li binary alloys," Acta metall. 30 (1982), 927.

8. Jha S.C., Sanders Jr T.H., and Dayananda M.A., "Grain-boundary precipitate free zones in Al-Li alloys," Acta metall. 35 (2) (1987), 473.

9. Brown L.M. and Ham R.K., Dislocation-particle interactions, in Strengthening Methods in Crystals, Kelly A. and Nicholson R.B., Editors. (Elsevier: Amsterdam, 1971) p. 9-135.

10. Meyers M.A. and Chawla K.K., Mechanical metallurgy: Principles and Applications. (Englewood Cliffs: Paramus, NJ, 1984), 343.

11. Frost H.J. and Ashby M.F., Deformation Mechanism Maps. Pergamon ed. (Oxford: Pergamon Press, 1982)

12. Nembach E., Particle Strengthening of Metals and Alloys: John Wiley, 1997)

13. Cadek J., Creep in Metallic Materials (Elsevier: New York, 1998)

14. Srolovitz D.J., Petrovic-Luton R.A., and Luton M.J., "Diffusionally modified dislocation particle elastic intercations," Acta mater. 32 (1984), 1079.

15. Harada Y. and Dunand D.C., "Creep properties of Al3Sc and Al3(Sc,X) Intermetallics," Acta mater. 48 (13) (2000), 3477.

16. Marquis E.A., Seidman D.N., and Dunand D.C., "Precipitation strengthening of heat-treatable Al(Sc) alloys at ambient and elevated temperatures," in preparation. (2001)

17. Murray J.L., "The Al-Sc (aluminum-scandium) system," J. Phase equilibria. 19 (4) (1998), 380.

18. Martin J.L., Creep of Pure Metals, in Creep Behaviour of Crystalline Solids, Wilshire B. and Evans R.W. (eds.), (Pineridge Press Press: Swansea, 1985) p. 1.

19. Blum W., in High-Temperature Deformation and Creep of Crystalline Solids. Mughrabi, H. (ed.) (VCH Verlagsgesellschaft: Weinheim, Germany, 1993), p. 359-405